

# Numerical Computation of Plunging Wave Impact Loads on a Vertical Wall. Part 2. The Air Pocket

Katsuji Tanizawa\* & Dick. K. P. Yue\*\*

\*Ship Dynamics Division, SRI, Shinkawa, Mitaka, Tokyo, Japan

\*\*Department of Ocean Engineering, MIT, Cambridge, Massachusetts, U.S.A.

## 1 Introduction

According to Chan & Melville (1988), the presence of trapped air plays an essential role in the plunging wave impact on a vertical wall. Thus, one expects the air pressure to be an important scaling factor and that its cushioning effect cannot be neglected in the study of water impact. A direct confirmation of trapped-air effects can, in principle, be obtained in a decompressible wave tank by varying the atmospheric pressure, thus effectively changing the scale of the air pocket effect. It is desirable, however, to obtain an estimate of these effects by numerical simulations before such expensive experiments are attempted. The present work concerns the numerical simulation of plunging wave impact on a vertical wall in the presence of a trapped air pocket.

At the previous workshop (Tanizawa & Yue 1991), we presented the mathematical formulation and numerical implementation for the simulation of wave impact in a two-dimensional rectangular tank with a piston wavemaker at one end. Numerical results were shown for the case without air. From those results, we concluded that the peak impact pressure, while sensitive to numerical discretization, nevertheless resulted in an impulse small compared to experimental measurements and to what one could expect from the effect of a trapped air pocket.

Encouraged by this success, we extend the work to include the effects of an air cushion and attempt a direct comparison to the measurements of Chan & Melville (1988). The basic assumptions of the numerical model are that the fluid is homogeneous, inviscid and incompressible, and that the flow is two-dimensional and irrotational and thus can be given by a complex velocity potential  $\beta$ . For the air pocket, the process of air compression is assumed to be uniform, adiabatic and described simply by a polytropic gas law:  $pv^\gamma = \text{constant}$ , where  $p$  is the trapped-air pressure,  $v$  the trapped-air volume, and  $\gamma=1.4$  for air is the ratio of specific heats. A mixed Eulerian-Lagrangian is used, and the boundary-value problem for  $\beta$  is solved at each time step using a boundary-integral method.

## 2 Numerical Results

Figure 1 shows a schematic of the numerical simulation in a two-dimensional tank. For simplicity, the problem is made dimensionless by setting the initial depth of the fluid in the tank  $h$ , the fluid density  $\rho$ , and gravitational acceleration  $g$  all to unity. A plunging

breaker is generated by an impulsively started constant forward motion ( $U=0.7$ ) of the piston wavemaker. The far wall is located at  $\ell=5.8$ . This wall is submerged to only half the mean depth to allow a gap  $y \in [-0.5, -1]$ . Inside this gap, an outflow boundary condition is applied which allows the size of the air pocket to be effectively adjusted.

Figure 2 shows a sequence of the surface contours of a plunging breaker generated this way. The last free-surface profile, indicated by a thickened line, is taken at the instant just after impact at which time a small portion (much less than order of panel size) of the plunger tip that crossed the wall is truncated. For the continuing simulation with the trapped air pocket, a range of different initial air pressures, which defines the physical scale of the problem, is considered:  $p_{atm} = 1, 10$  and  $100$ . The development of the free surface subsequent to the profiles in Figure 2 for  $p_{atm} = 1$  and  $100$  are shown in figures 3 and 4 respectively.

Despite very small panel sizes ( $\Delta\ell \sim .01$ ) in the impact region to maintain fine spatial resolution, the free surface inside the plunger remains stable in all cases even in the expansion phase of the air pocket in the  $p_{atm}=100$  case. The simulated air pocket profiles are smooth and appear realistic, with the effect of buoyancy clearly observable in the rising motion of the trapped air. We remark that no numerical smoothing are required in the simulations. A regriding scheme based on cubic-splines is used at each time step. Given the development of the air pocket geometry, the time history of the air pressure in the pocket is easily obtained under the assumptions of a polytropic gas law.

The time history of the trapped-air pressure for different values of  $p_{atm}$  are given in figure 5. Of particular interest is the case of  $p_{atm} = 100$  where the bubble oscillation reaches a peak air pressure amplitude of  $\sim 22$  times the maximum hydrostatic pressure  $\rho gh$ . In this case, the total peak impact force is  $F/\rho gh^3 \sim 4.6$  and the total impulse  $I/\rho h^3 \sqrt{gh}$  reaches a value of  $\sim 0.1$ .

We now turn to comparisons between our numerical predictions and actual tank measurements.

### 3 Comparison between simulation and experiments

To facilitate a direct comparison to measurements, it is necessary to first define a characteristic velocity  $C$  for the plunging wave. In the experiments of Chan & Melville, the plunger was generated by focussing a wave packet and  $C$  was taken to be the (linear) phase velocity of the central component. Corresponding approximately to this value, we take as the characteristic velocity that at the plunging wave tip just before impact. From the numerical simulation, this value is given by  $C \cong 1.96$ .

Table 1 gives an order of magnitude comparison between the experimental values and the numerical predictions based on the simulation case of  $p_{atm} = 100$ . Using the value of  $p_{atm}=10^5$  N/m<sup>2</sup>,  $\rho=10^3$  kg/m<sup>3</sup>, and  $g=10$  m/s<sup>2</sup>, we calculate a value of  $h \sim 10$  cm, yielding an initial air pocket dimension of  $\sim 3$  cm. From figure 4 of Chan & Melville, we estimate their corresponding bubble dimension to be  $\sim 1$  cm. Thus our  $p_{atm} = 100$  case corresponds approximately to the experimental scale.

Assuming this to be the case, the comparison between the predicted and measured peak impact pressure is quite satisfactory. The computed peak air pressure of  $\sim 22\rho gh \cong 6\rho C^2$ ,

while the measured impact pressures range from  $6 \sim 10\rho C^2$ . In view of the different sizes of the air pocket, the agreement for the impact duration is also acceptable. The experimental oscillation frequency in the impact pressure is reported to range from  $0.3\sim 5$  kHz corresponding to a impact duration of  $1.5\sim 0.1$  ms. On the other hand, the computed impact duration of 0.03 from figure 5 gives a physical value of 3 ms.

Further details of trapped-air impact with various scales as well as scaling laws accounting for the air pocket will be discussed.

## 4 References

Chan, E. S. & Melville, W. K., 1988, Deep-water plunging wave pressure on a vertical plane wall. *Proc. R. Soc. Lond. A* 417.

Tanizawa & Yue, 1991, Numerical Computation of Plunging Wave Impact Loads on a Vertical Wall. *Proc. 6th Intl. Workshop on Water Waves & Floating Bodies*.

Table 1. Comparison between measurements and simulation.

	Experiments (Chan & Melville 1988)	Computations $p_{atm}=100\rho gh$
Dimension of air pocket	$\sim 1$ cm	$\sim 3$ cm
Maximum impact pressure	$6\sim 10 \rho C^2$	$6\rho C^2$
Duration of impact pressure	$0.1\sim 1.5$ ms	3 ms

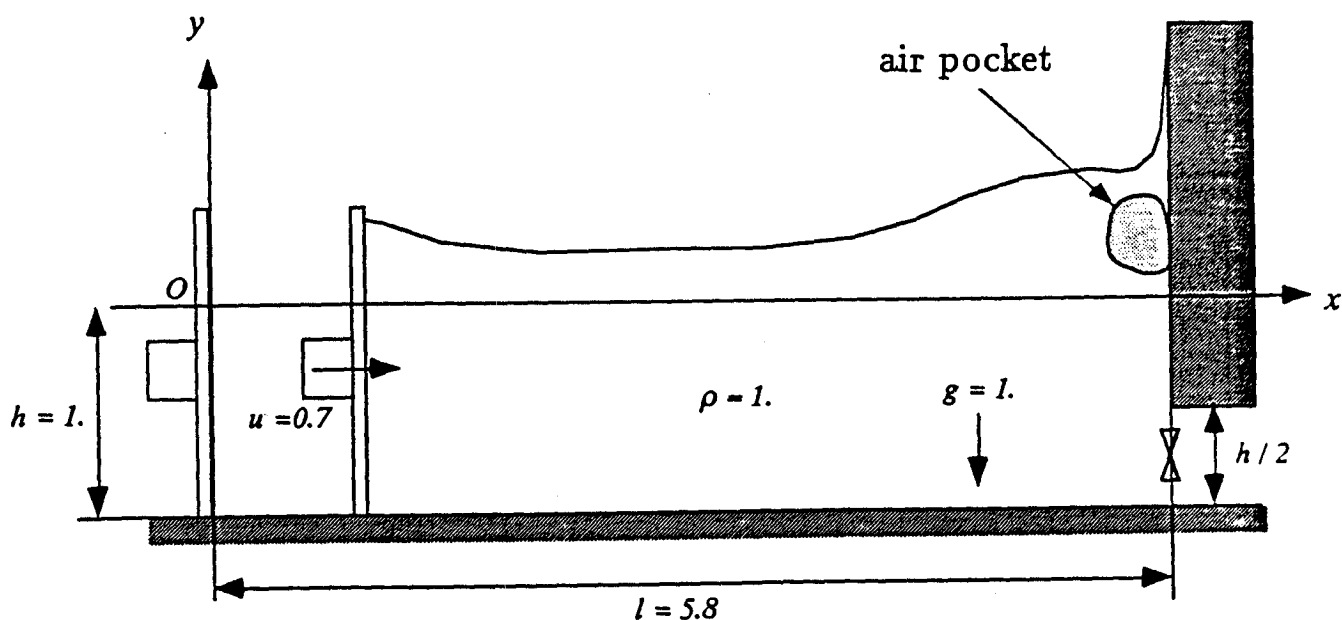


Fig.1 Sketch of the simulation

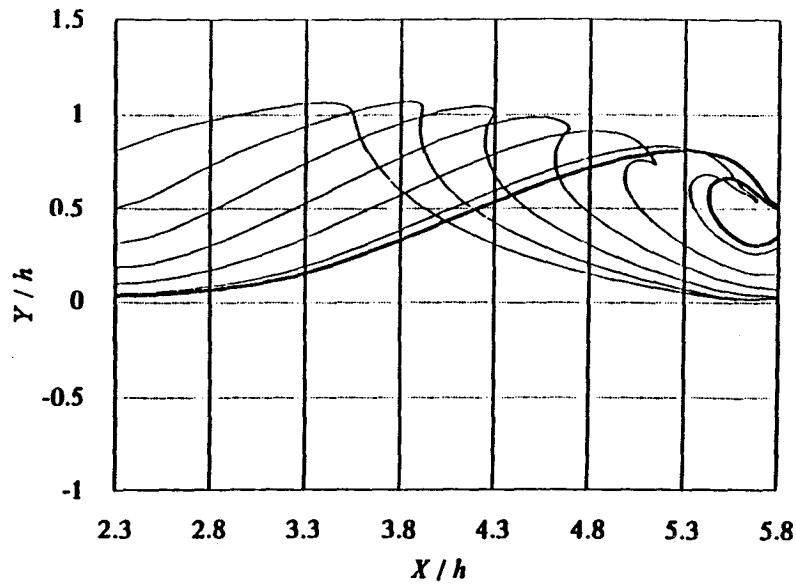


Fig.2 Free-surface profile of the simulated plunging wave.

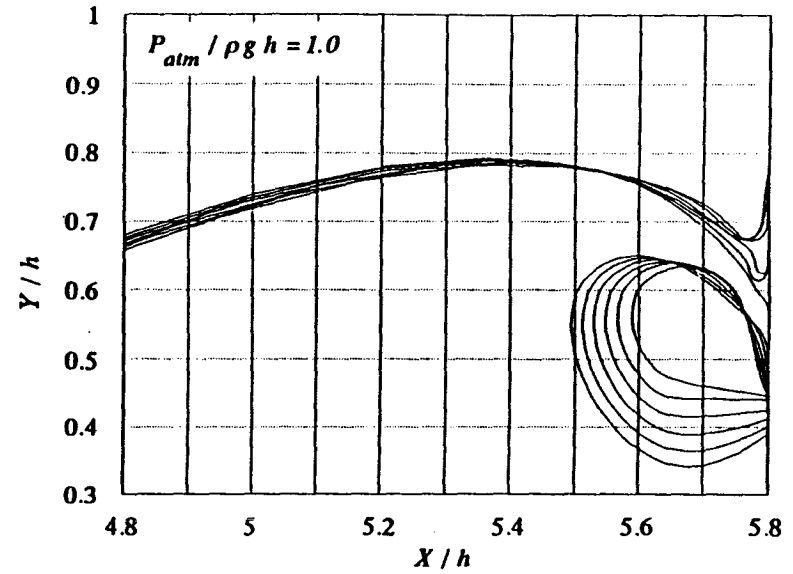


Fig.3 Free-surface profile of the simulated plunging wave impact.

$T(g/h)^{1/2} = 0, 0.01, 0.02, 0.03, 0.04, 0.05$

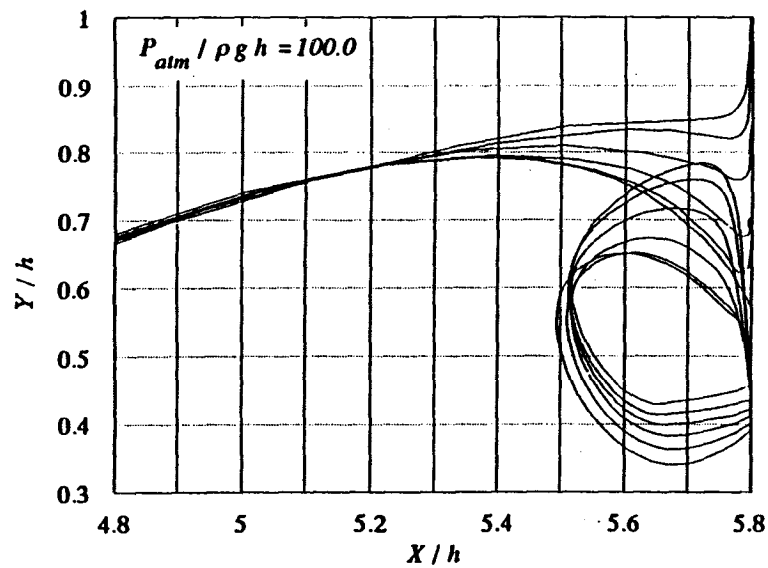


Fig.4 Free-surface profile of the simulated plunging wave impact.

$T(g/h)^{1/2} = 0, 0.01, 0.02, 0.03, 0.04, 0.05$

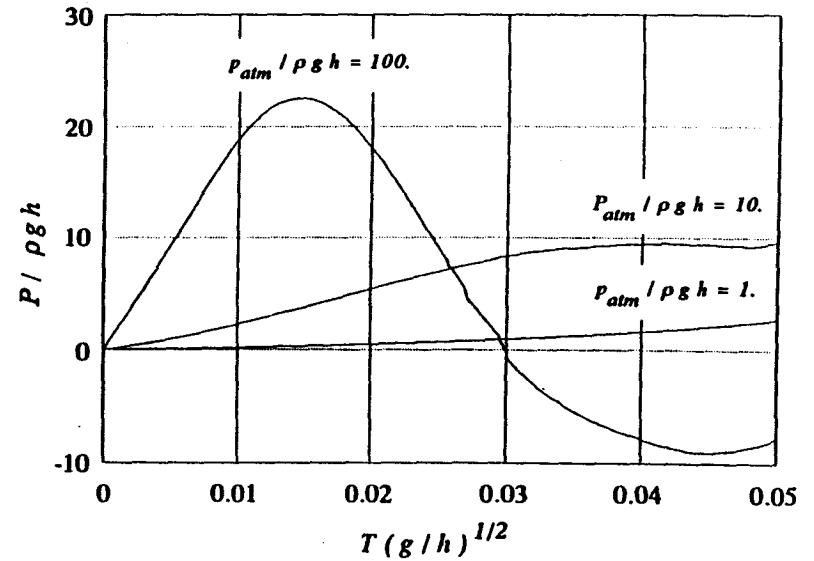


Fig.5 Calculated trapped-air pressure between vertical wall and plunging breaker

## DISCUSSION

**GREENHOW:**

1) Cooker (Manchester Workshop) has shown that waves which impact on a wall before overturning can also give extremely high pressures due to the  $\frac{\partial \phi}{\partial t}$  term.

2) For initial jet impact, you may be able to use self similar flows, as in Cumberbatch (1960 *J. Fluid Mech.*) and in Gurevich's book on jets and cavity flows.

**TANIZAWA & YUE:**

1) Cooker has shown the existence of high acceleration field at the root of the upwashing flow. But it does not mean the existence of high pressure. It only means the existence of large pressure gradient. Since the scale of high acceleration field is very small, the pressure itself is not so high.

2) We thank Dr. Greenhow for pointing out the references. The work by E. Cumberbatch (JFM 1960), in particular, is most relevant to our simulation of the jet at initial impact and may provide a useful "inner" solution to the problem.

**BROEZE:** With a potential flow model, the moment of first impact cannot be modelled due to infinite pressure. During the first moments of impact, the pressure in the jet at the wall is much larger than it becomes in the air pocket at larger times.

What is the use of these pressure computations with a potential flow method, if they cannot provide the largest pressure impacts?

**TANIZAWA & YUE:** The peak impact pressure of the water impact is certainly higher than that of the air impact. But, the water impact pressure acts on much smaller area compared with the trapped air pressure. And its duration is also much shorter than the air impact duration. In consequence, total impulse of the air impact pressure becomes larger than that of water impact. We consider that the total impulse is more important for the design of ocean structures.

**SCHULTZ:** Since the transition from stage 1 to stage 2 violates the continuous mapping, what model do you use for the transition and how does it affect the results?

**TANIZAWA & YUE:** We perform a truncation as soon as the first Lagrangian point crosses the wall in the time integration. Since our time steps are dynamically controlled so that a Lagrangian point can move only a small fraction (typically  $\alpha \approx 10\%$ ) of the smallest panel size, the truncated volume, fluid momentum etc. are scaled by (a small fraction of) the panel size. For global spatial and temporal behavior, we are able to obtain convergence with diminishing  $\alpha$ . The convergence of our results for the spatial and temporal limiting peak pressure at the point of impact is, of course, a different matter and is a subject of current investigation.

**CAO:** Can you explain how the outflow boundary condition inside the gap between the wall bottom and the bottom of the tank adjusts the size of the air pocket? What kind of outflow boundary condition do you use? Can the outflow condition you use easily be controlled in an experiment?

## DISCUSSION

TANIZAWA & YUE: The "outflow" on the bottom half of the wall is controlled by specifying a given flux rate (in fact the stream function variation in a Cauchy integral formulation). This is done to allow us to range the air pocket size without resorting to much long tank and more complicated wave maker motion. In later simulations and experiments, a 'full' tank and composite wave maker motions (e.g. Chan & Melville, 1989) will/can be used to develop the desired plunging wave.